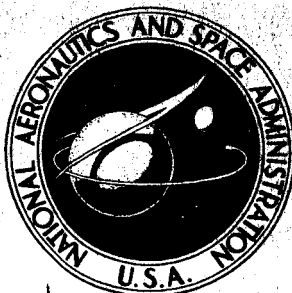NASA CONTRACTOR
REPORT

NASA CR-701

NASA CR-701

GFO PRICE $ _____

CFSTI PRICE(S) $ __2.00__

Hard copy (HC) _____

Microfiche (MF) __.65__

FACILITY FORM 602

N67-15670
(ACCESSION NUMBER)   (THRU)

32
(PAGES)   (CODE)

CR-701
(NASA CR OR TMX OR AD NUMBER)   (CATEGORY)

STUDY OF HOT-CATHODE
MAGNETRON ION GAUGE

by J. M. Lafferty, W. D. Davis, and L. J. Favreau

Prepared by
GENERAL ELECTRIC COMPANY
Schenectady, N. Y.
for Goddard Space Flight Center

NATIONAL AERONAUTICS AND SPACE ADMINISTRATION • WASHINGTON, D. C. • JANUARY 1967

STUDY OF HOT-CATHODE MAGNETRON ION GAUGE

By J. M. Lafferty, W. D. Davis, and L. J. Favreau

Distribution of this report is provided in the interest of information exchange. Responsibility for the contents resides in the author or organization that prepared it.

NATIONAL AERONAUTICS AND SPACE ADMINISTRATION

ABSTRACT

A study was made of the problems associated with the operation and calibration of vacuum gauges at pressures below 10^{-10} torr, particularly the hot-cathode magnetron gauge as developed by Lafferty. Under proper operating conditions, the output of this gauge was linear with pressure to 3×10^{-12} torr with indications of normal behavior to at least 1×10^{-12} torr. Considerable information was also obtained on a commercial cold-cathode magnetron or discharge gauge. Calibration at lower pressures is limited at present by the system base pressure.

The possibility of developing a high output ion source for a quadrupole mass spectrometer using the hot-cathode magnetron principle also was explored. Sensitivities of 1 to 5×10^{-3} amp/torr were obtained for a suitably focused ion beam, but a more extensive determination of the stability of the source, the energy spectrum of the ion beam, and the requirements of the mass analyzer are necessary before the maximum output can be stated.

TABLE OF CONTENTS

LIST OF ILLUSTRATIONS

LIST OF SYMBOLS

P_1 Pressure in calibration manifold (torr).

P_2 Pressure in pumping manifold (torr).

Q   Gas flow rate through system (liter-torr/sec).

C_1 Conductance for gas flow into calibration manifold (ℓ/sec).

C_2 Conductance for gas flow out of calibration manifold (ℓ/sec).

S   Pumping speed of liquid He pump (ℓ/sec).

P_M Pressure measured by McLeod gauge (torr).

P_1^0 Initial pressure in calibration manifold (torr).

P_2^0 Initial pressure in pumping manifold (torr).

M   Mass number.

STUDY OF HOT-CATHODE MAGNETRON ION GAUGE

J. M. Lafferty, W. D. Davis, and L. J. Favreau

I. GAUGE CALIBRATION

A. Introduction

Essentially all the practical gauges for pressures in the ultrahigh vacuum range measure the current produced by ionization of the molecules. None can be considered as absolute gauges in the sense that their output as a function of pressure can be accurately calculated. In addition, various effects such as x-ray induced photoemission or electronic ion desorption from surfaces may contribute spurious currents. Discharge type gauges are generally plagued with an output which is not only nonlinear with pressure but which also changes its degree of nonlinearity with changes in pressure. Therefore, for reliable pressure measurements all gauges need to be calibrated by some absolute method, especially if the measurements are to be extended below 10^{-10} torr. The gauge of primary interest in this investigation is a hot-cathode magnetron developed by Lafferty.[1,2] The hot-cathode magnetron uses a magnetic field to greatly increase the path length of the ionizing electrons emitted by a hot filament. This greatly increases the sensitivity of the gauge without at the same time increasing the x-ray level. Lafferty found that the calculated x-ray current corresponded to a pressure of 4×10^{-15} torr for 1×10^{-9} amp emission or 1.5×10^{-14} torr for 1×10^{-7} amp emission. However, the low-pressure limitations of the gauge have not been determined experimentally.

Calibrations of vacuum gauges at pressures below 10^{-10} torr have not been numerous or extensive. This is primarily due to the difficulty of lowering the background pressure well below the calibration pressure rather than in producing known pressure increments of pure gases. The latter is usually accomplished by establishing a known rate of flow of gas into the calibration region and a known pumping speed or conductance out of the region. However, even this process becomes more difficult as one progresses from an inert nonadsorbing gas such as He to an active gas such as O_2.

Feakes and Torney[3] obtained pressures estimated to be below 10^{-15} torr by using a combination of oil-diffusion pumping and cryopumping. Known He partial pressures were established using two calculated conductances and a calibrated ionization gauge to measure the upstream pressure. Because the chamber was cooled to 10°K while the gauge was at 175°K, only He could be used and rather large and uncertain temperature corrections were necessary. A Redhead type cold-cathode magnetron gauge was calibrated down to about 4×10^{-13} torr (not fully corrected).

Bryant and co-workers[4] used a similar procedure to obtain He pressures in the 10^{-12} torr region but apparently did not need to cool the test region to obtain sufficiently low base pressures. The operational characteristics of a Redhead gauge and a similar type gauge developed by Kreisman were obtained.

Kreisman[5] used Hg diffusion pumps on a glass system to obtain base pressures in the 10^{-13} torr region. Developmental cold-cathode magnetrons were calibrated down to the 10^{-12} torr region using He or N_2 flow through a standard glass capillary tube. A Bayard-Alpert gauge was used to measure the upstream pressure.

B. Method of Calibration

The method used in this investigation to obtain known pressures of pure gases is essentially the same as that used in earlier work.[6] It is based on the familiar relationship $P_1 - P_2 = Q/C_2$ (see Fig. 1) where P_1 is the pressure in the calibration volume, P_2 is the pressure on the low-pressure side of the conductance, C_2, and Q is the gas flow introduced into the system. The conductance C_2 is a large orifice in a plate and its value can be calculated. P_2 is approximately equal to Q/S where S is the speed of the liquid He pump. If S is large compared to C_2, P_2 will be small compared to P_1 and hence need not be known accurately. P_2 is measured with a hot-cathode magnetron which is calibrated by comparison with its mate in the calibration volume for conditions of little or no flow across C_2(cryogenic pump at room temperature). Q is determined by the relationship $Q = P_M C_1$ where P_M the upstream pressure, is measured by a McLeod gauge and C_1, a long narrow capillary, is calculated from its dimensions. C_1 can also be determined by measuring the flow rate of gas at atmospheric pressure into the leak valve for various steady-state pressures on the McLeod gauge. Various methods may be used for this purpose, the simplest perhaps being the measurement of the motion of a mercury pellet along a small calibrated pipette. This simple method gives results accurate to within a few per cent for flow rates of 10^{-4} std cc/sec or greater. Previous measurements of this kind with a glass capillary 1 mm in diameter and 10 cm long for C_1 gave results for the conductance which agreed with the calculated value to within the accuracy of the method (calculated = 1.20 cc/sec, measured = 1.22 cc/sec).

The absolute accuracy of the method thus depends primarily on the accuracy of the calculated conductances C_2 and C_1 and the measured pressure P_M. If direct flow measurements are made, however, the accuracy will depend only on C_2 and the accuracy of the flow measurements.

The foregoing treatment, however, applies only for gas flows sufficiently high to cause pressures P_1 and P_2 to be much greater than their respective base pressures, P_1^0 and P_2^0. In order to extend the calibration to the lowest possible pressure, suitable corrections must be made. The method chosen is based on the assumption that the added flow of calibration gas does not disturb the original steady-state conditions of outgassing and pumping that determined the base pressures. In other words, the calibration pressures merely add to the base pressures. If this is the case:

$$(P_1 - P_1^0) - (P_2 - P_2^0) = Q/C_2 .$$

Usually, P_1^0 and P_2^0 were approximately equal and this correction was small.
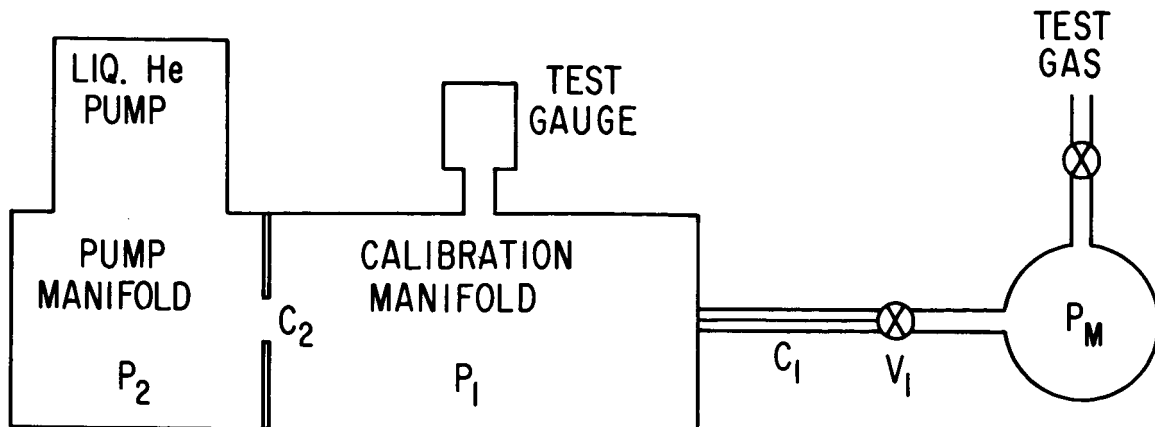
Fig. 1 Schematic drawing of calibration system showing method used.

C. Calibration System

The calibration manifold and cryogenic pump are shown in Figs. 2 and 3. The chief material used for fabrication was stainless steel. The various parts were joined with stainless steel flanges and copper gaskets. Except for the mass spectrometer, no glass was used in this area in order to avoid a large He background by diffusion from the atmosphere. Pumping during bakeout and standby operation was supplied by a 3-stage glass mercury diffusion pump and liquid N_2 trap with a net pumping speed of about 15 l/sec for N_2. The 1 1/2-inch metal valve (V_2) and associated piping that separates this pumping system from the cryogenic pumping manifold reduces the speed at the manifold to about 5 l/sec. The intended function of the 25 l/sec triode ion pump attached to the pumping manifold was primarily to pump any gas not pumped efficiently by the cryogenic pump--chiefly He and H_2. It turned out, however, that the liquid He pump pumped all gases, even He, while the speed of the ion pump at very low pressures was much less than the rated value. When the liquid He pump was in use, the ion pump had no apparent effect on the ultimate pressure. The measured speed of the ion pump for He at about 1 x 10^{-10} torr was 1.5 l/sec while the speed through the 1 1/2-inch valve was about 15 l/sec. For H_2, the corresponding speeds were 12 and 17 l/sec. As a consequence, use of the ion pump was discontinued.

The design of the liquid He cryogenic pump is shown in Figs. 4, 5, and 6. Based on the area of liquid He cooled surface alone and assuming a sticking probability of 1.0, the speed for N_2 would be about 900 l/sec. The measured speed with the baffle added was about 300 l/sec. Earlier, a chevron-type baffle across the baffle support opening had been tried but the measured speed was only about 190 l/sec. Although one might suspect that the more open structure of the higher speed baffle would allow more radiant heat to reach the liquid He can, the pumping time for both arrangements was 3 to 3 1/2 hours. One disadvantage, however, is that with the extended baffling structure, the requirement that P_2 be a well-defined pressure produced by molecules with a random room-temperature velocity distribution is probably not met exactly.

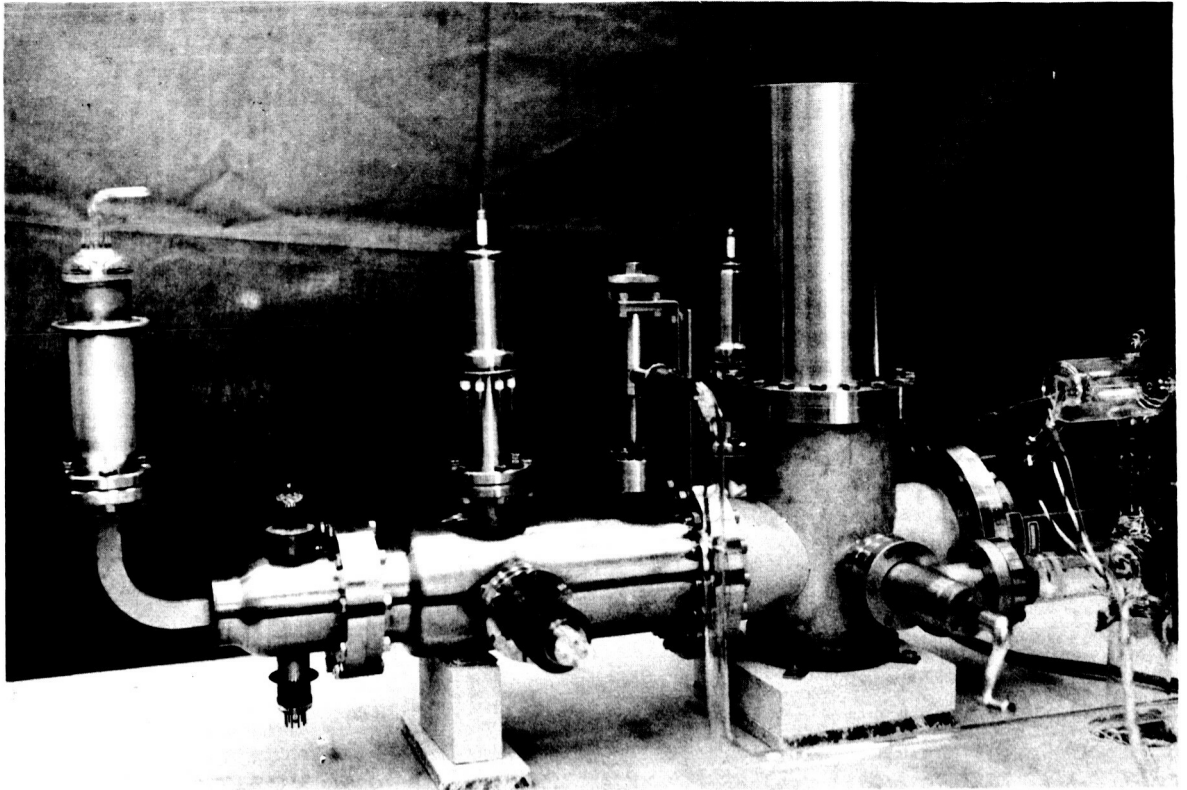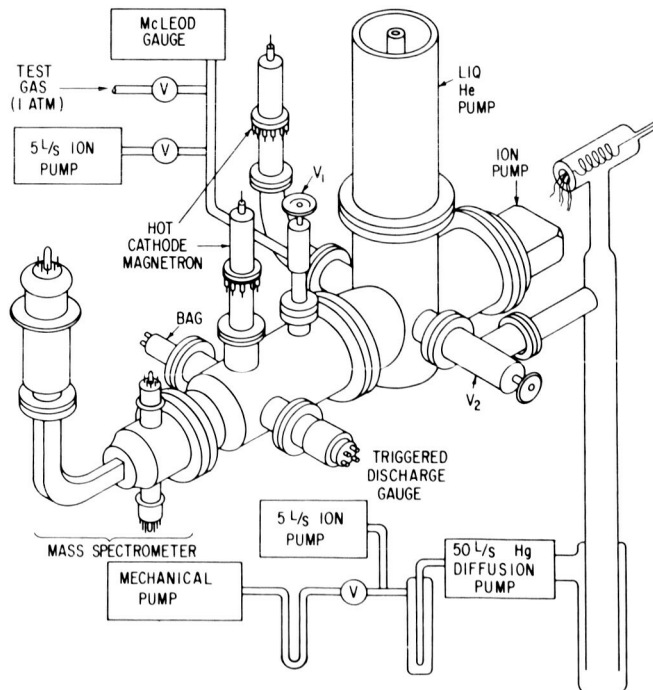Fig. 2 Photograph of main portion of calibration system on bakeout table.

Fig. 3 Drawing of complete calibration system. The three traps shown at the bottom were cooled with liquid N_2.
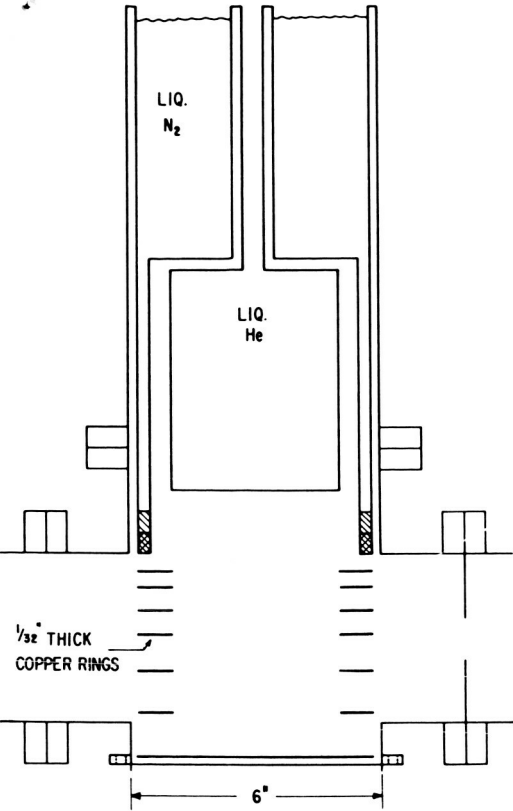
Fig. 4 Construction of liquid He pump and liquid N_2 cooled heat shield.

LIQ. N_2

LIQ. He

$\frac{1}{32}$" THICK
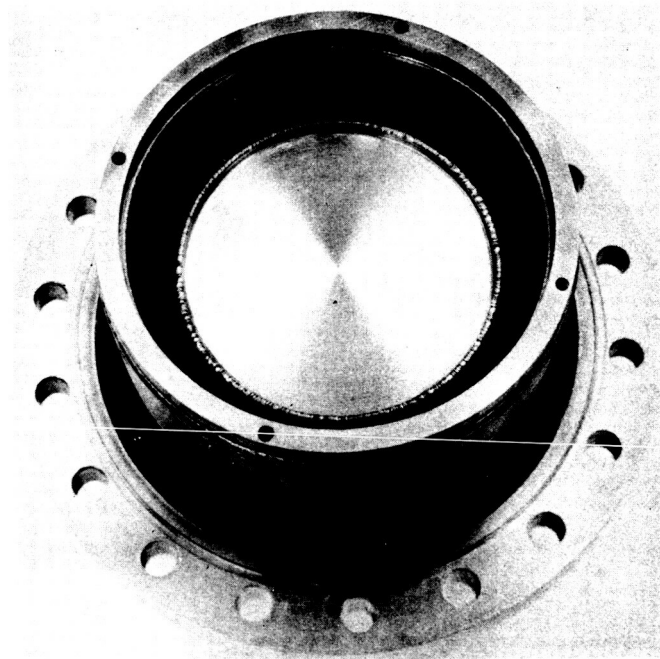COPPER RINGS
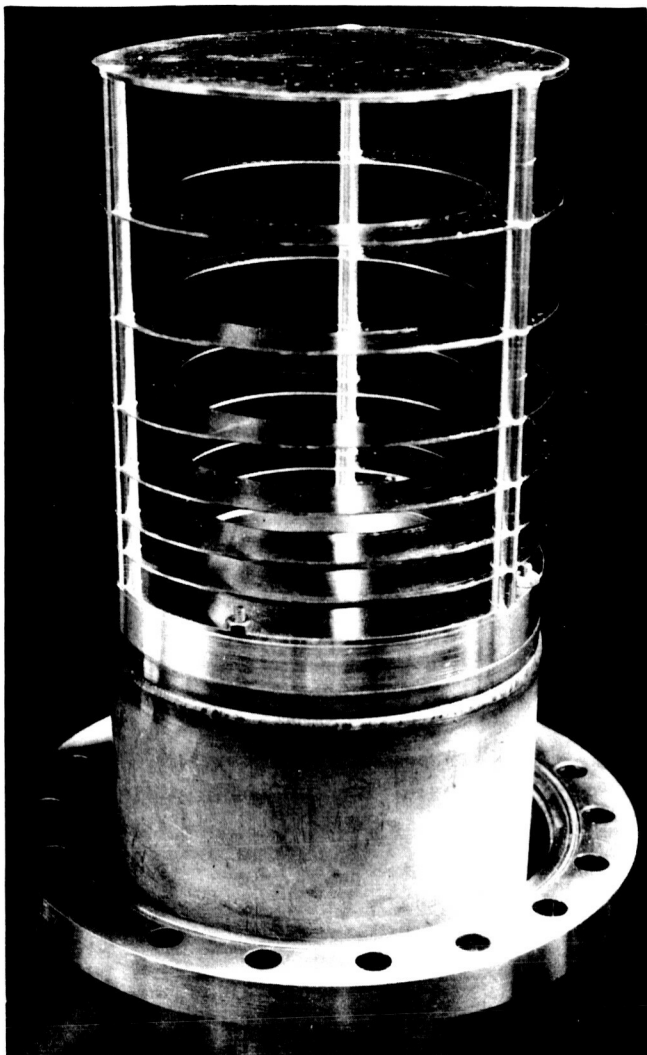
6"

Fig. 5 Photograph of lower end of liquid He pump with baffle removed.

Fig. 6 Photograph of lower end of liquid
He pump with baffle in place. The three
rods are 6.33 mm (1/4 inch) copper rod.

The orifice C_2 is a 2-cm-diameter hole in a stainless steel disk brazed to the copper gasket used for the large end flange of the calibration manifold. It has a calculated conductance of 37.3 ℓ/sec for N_2 at 25°C. This choice for C_2 is a compromise between the need for high pumping speed in order to achieve low ultimate calibration pressures and the desirability of having a high P_1/P_2 ratio in order to minimize the P_2 correction term. The measured P_1/P_2 ratio is approximately 10 so that a 10% error in P_2 produces only a 1% error in P_1. The gas inlet conductance, C_1, is a 1.110-mm-diameter stainless steel tube, 10.02 cm long, with a calculated conductance of 1.665 cm^3/sec. At the conclusion of the low-pressure calibration, flow measurements will be made to check the accuracy of this value. One end of C_1 is brazed onto the upper gasket of the flange joining the inlet valve V_1 and the calibration manifold. The other end terminates near the bottom of the manifold. In this position, it is assumed that the gauges and the orifice C_2 will "see" only molecules that have been sufficiently randomized by collision with the walls of the manifold.

The McLeod gauge used to measure the gas inlet pressure P_M is a CVC model GM-100. The manufacturers' accuracy based on an estimated reading error of ± 0.25 mm varies from $\pm 3\%$ at 10^{-3} torr to $\pm 0.3\%$ at 10^{-1} torr. The ratio P_M/P_1 is 2×10^4 so that assuming the lowest accurate value of P_M is 10^{-3} torr, this system of conductances allows one to calibrate down to 5×10^{-8} torr. With care, results another decade lower can be obtained without excessively large errors.

For lower pressures, the metal valve leading to C_1 is throttled down so that it becomes the limiting conductance. With this smaller conductance, much lower flow rates can be used and still maintain the pressure in the McLeod gauge within a readable range. The conductance of the valve was determined by increasing the pressure on the McLeod side until the pressure in the calibration manifold reached the lower part of the previously calibrated pressure region. For example, if the calibrated small

orifice required 10^{-2} torr on the McLeod to produce a certain reading on the ionization gauge and the throttled valve required 1 torr to give the same reading, the ratio of the two conductances must be 100 to 1. The only assumption required for this calculation is that the flow through the throttled valve be true molecular flow. This is certainly to be expected from the consideration of the molecular mean free path at the pressures involved and the characteristic dimensions needed to give the observed flow rates. The best evidence, however, is the agreement in the gauge calibration for pressures considerably above the minimum pressure needed for calibrating the throttled valve.

The gauges to be studied included the hot-cathode magnetron, a Bayard-Alpert type ionization gauge (BAG), a cold-cathode magnetron or discharge gauge and a mass spectrometer. The construction of the hot-cathode magnetron gauges is shown in Figs. 7 and 8 and is similar to those described by Lafferty.[1,2] A hairpin cathode of 0.13 mm Re electrophoretically coated with LaB_6 is used. The magnetic field is about 290 gauss. The cold-cathode gauge is a so-called "Triggered Discharge Gauge" manufactured by the General Electric Company, Model 22HF100. A small W filament is used to start the discharge between the cylindrical anode and the two end plates used as ion collectors. The axial magnetic field is about 1000 gauss and the anode voltage is 2 kv. The Bayard-Alpert type hot-cathode ionization gauge is a GE Model 22GT114. This particular model was chosen because it was of metal-ceramic construction and could be flange mounted. It used both a W filament and a ThO_2 -Ir filament.

The mass spectrometer is a 5 cm radius of curvature 90° magnetic deflection type instrument of conventional design. Similar instruments have been used in previous work[7,8] and offer high sensitivity for determining gas composition at very low pressures. Although not designed for the precision and stability of the large commercial instruments, it usually provides reliable partial pressure values if care is used in its operation. Its primary purpose is to aid in the attainment of low base pressures, both by analyzing the residual gas and serving as an extremely sensitive leak detector. It is also helpful in analyzing the calibration data obtained at pressures near the base pressure or for active gases such as O_2. The ion source incorporates two hairpin-type filaments to produce electrons--one of 0.10 mm tungsten wire and the other of 0.13 mm Re wire tipped with LaB_6. The ions are accelerated to approximately 1000 volts, analyzed with a 0 to 10 kG electromagnet and detected with a high-gain 10-stage electron multiplier.

ION COLLECTOR

ANODE

5 MIL RHENIUM FILAMENT
(LaB_6 COATED)
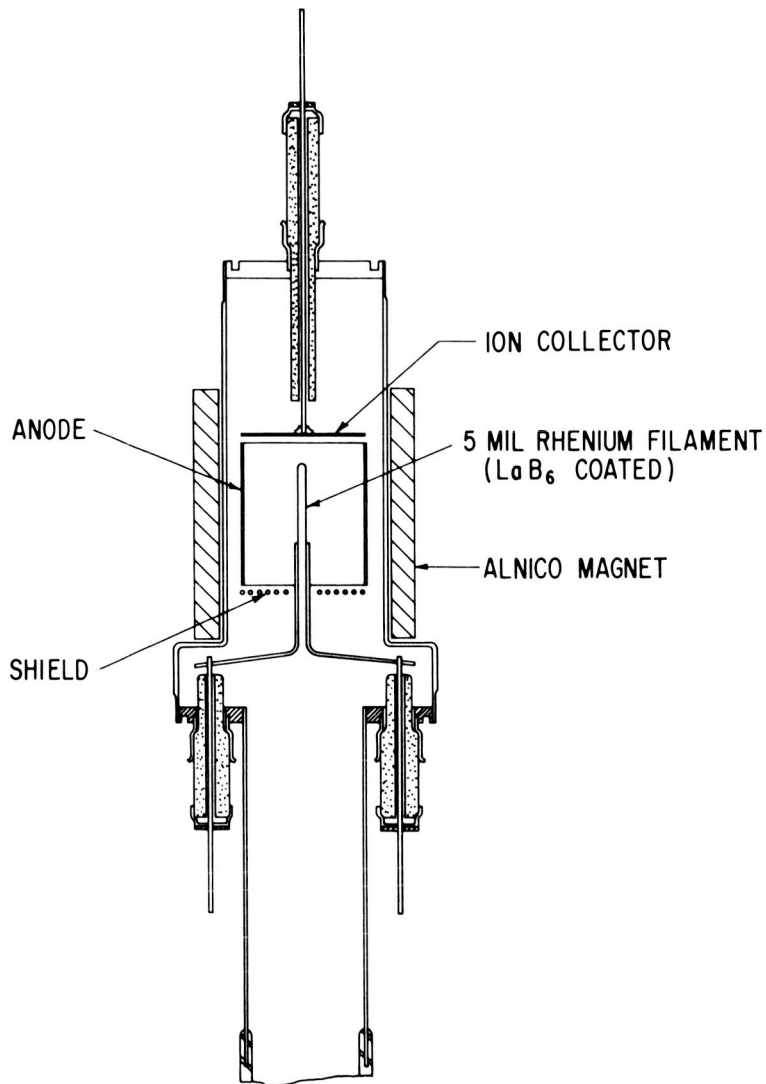
ALNICO MAGNET

SHIELD

Fig. 7 Cross-sectional view of hot-cathode
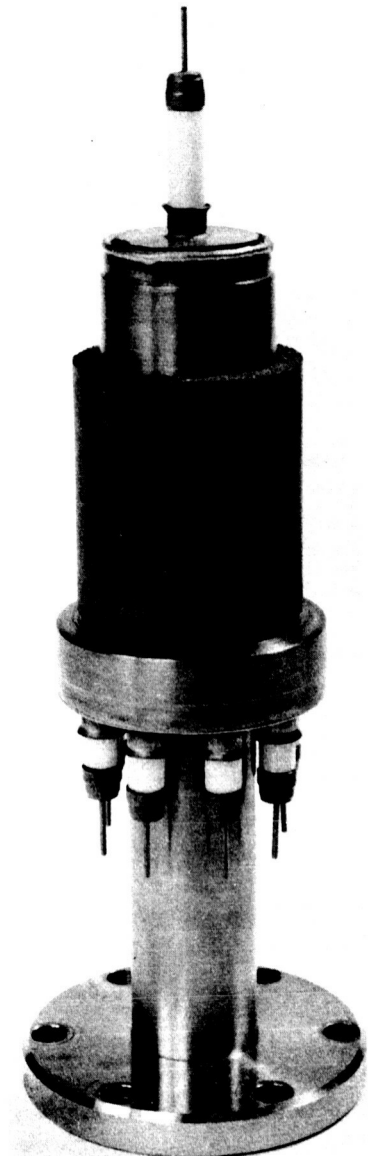magnetron gauge.

Fig. 8 Photograph of the hot-
cathode magnetron with
magnet in place. The tubu-
lation is 2. 5 cm in diameter
by 8 cm long.

-8-

D. System Performance

The initial bakeout of the system at 400°C for 24 hours revealed a fairly large amount of contamination in the system. The electron multiplier had low gain and high electrical leakage in spite of the use of $CsNO_3$ for activation. In addition, the 1 1/2-inch valve had a leak to the atmosphere on the Hg pump side of the seat which necessitated applying an external rough vacuum to reduce the pressure below 10^{-8} torr.* The base pressure with the Hg diffusion pump but without liquid N_2 in the radiation shield was about 2×10^{-9} torr with approximately equal pressures of mass 28 (N_2 + CO) and H_2. Adding liquid N_2 decreased both components but after a few hours, the cold pumping surface would become saturated with H_2 and the H_2 pressure would be essentially as before. The mass 28 pressure (mainly N_2) would, however, remain low at about 7×10^{-11} torr. Addition of liquid He, in contrast, would greatly reduce the H_2 pressure but have only a relatively minor effect on mass 28. A typical base pressure of about 5×10^{-11} torr consisted of about equal pressures of mass 28 and H_2. In spite of the difficulties mentioned, calibration runs were made to evaluate the over-all performance of the system. All gauges responded normally and reproducible results were obtained. Equilibrium on changing the flow rate was established in less than 1 minute and no hysteresis effect was observable.

The system was opened to air and the faulty 1 1/2-inch valve previously mentioned was replaced. The electron multiplier was reactivated on a separate vacuum system and replaced. After a bakeout of 420°C for 24 hours, a pressure of 2×10^{-10} torr was obtained (50%-H_2, 50%-28). As before, addition of liquid N_2 reduced mass 28 while liquid He reduced H_2 with the resulting pressure of 1×10^{-11} torr being about equally divided between H_2 and 28. A low-temperature bakeout at 350°C for 24 hours with gradual temperature reduction over another 24 hours improved the vacuum by only about a factor of 2. A third bakeout at 420°C for 30 hours with more careful attention to temperature uniformity added another factor of 2 improvement.

The pressure in the calibration manifold was now about 6×10^{-11} torr at room temperature, 3×10^{-11} with liquid N_2 and 2×10^{-12} torr with liquid He. P_2 was about 5 to 6×10^{-13} torr. The mass spectrometer indicated equal pressures of H_2 and mass 28 at its normal operating emission of 100 μa but on reducing the emission to 10 μa, the indicated pressure of H_2 remained the same while the mass 28 pressure fell by a factor of 2. All tests indicated that the spectrometer was linear with emission so probably the effect was caused by local outgassing near the filament. The complete mass spectrum is shown in Fig. 9. Besides the major gas peaks of H_2 at mass 2 and N_2 + CO at mass 28,

---

*The pressure of the calibrating gas in any discussion of the calibration results is always expressed as the true pressure. All other pressures or partial pressures are expressed as equivalent N_2 pressure. True H_2 pressure $\approx 2.5 \times$ equiv N_2 pressure.
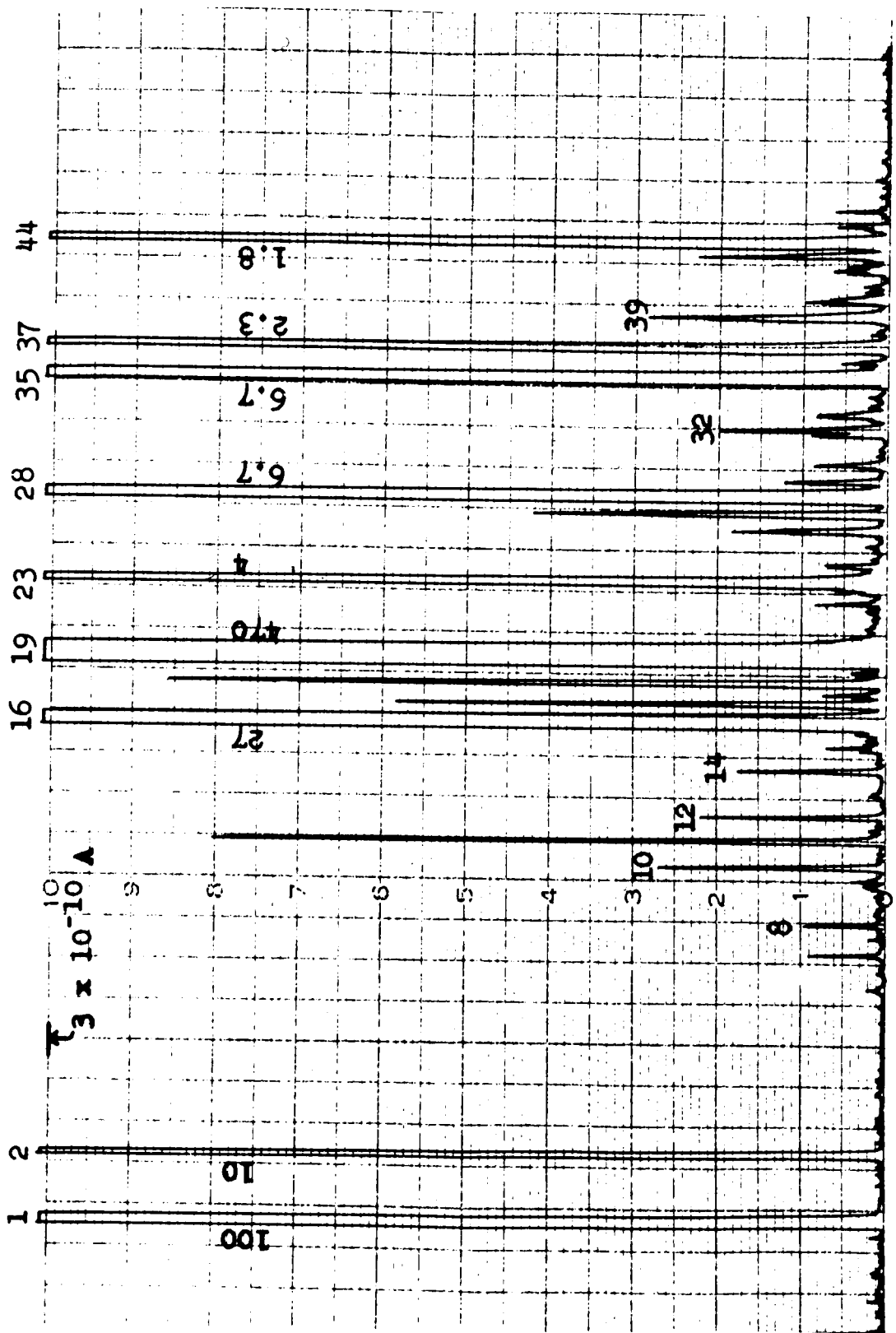
Fig. 9 Mass spectrum obtained at base pressure of system. Total pressure = 3×10^{-12} torr. Emission = 100 μa. Multiplier voltage = 1800 volts. Full scale on recording = 3×10^{-10} amp or 3×10^{-13} torr (N_2). Off-scale values in full-scale units (3×10^{-10} amp).

several large peaks due to ions produced by electron bombardment of surface impurities will be noticed. The major ones are mass 1 (H^+), 10 and 11 (B^+ deposited by LaB_6 filament), 16 (O^+), 19 (F^+), 23 (Na^+), and 35 and 37 (Cl^+). Mass 39 is probably K^+ while 26 and 27 (as well as some of the small peaks) are probably surface impurities of an organic nature. At the time this spectrum was obtained, the total pressure was somewhat higher than normal and the water peak (mass 18) was about 3X its normal value. Mass 17 is composed of about equal parts of OH^- from gaseous H_2O and a surface-derived ion which is presumably also OH^-. Efforts to determine the source of the residual gas were not successful. No leaks were detected. Mass 28 is probably due to outgassing of filaments and surfaces in general. Baking, exterior cooling and lower filament temperatures usually produced lower mass 28 pressure. The H_2 level however was much more stubborn and a likely source is diffusion from certain hydrogen-fired components that unfortunately were not vacuum fired before assembly.

E. Gauge Performance and N_2 Calibration

1. Bayard-Alpert Gauge

The primary difficulty with this gauge was the development of electrical leakage from the ion collector to ground. This necessitated keeping the gauge cool to increase the leakage resistance and the use of as low an input resistance in the electrometer as possible. Figure 10 shows two calibration curves for the Bayard-Alpert gauge using N_2. Exposure to air and bakeout at 420°C occurred between the two calibrations as discussed earlier. The circles on the lower curve were obtained with valve V_1 fully open while the squares were obtained with the valve throttled down so that its conductance (combined with C_1) was 1% of C_1. No correction was made for the x-ray or residual current of the gauge.

The residual current in the gauge could be determined quite readily by lowering the pressure to the 10^{-12} torr range and subtracting from the observed reading the small amount of ion current one could calculate should be present. Reproducible values could be obtained over a reasonable range of pressure. Before the last bakeout, the residual current corresponded to 0.74×10^{-10} torr. After the last bakeout, it had increased to a value corresponding to 1.2×10^{-10} torr. By correcting the gauge readings, for this residual current, a linear calibration curve for the BAG could be extended down to about 10^{-11} torr, as shown in Fig. 11.

2. Hot-Cathode Magnetron

The initial operating conditions for the hot-cathode magnetron were filament +45 volts, shield +35 volts, anode +345 volts and ion collector grounded with an emission of 1×10^{-7} amp before magnetic cutoff. The lower curve of Fig. 12 shows the calibration obtained under these conditions for high pressures and before the faulty valve was replaced. The nonlinearity above 10^{-8} torr is typical of these gauges. After the system was repaired, baked out and the gauges outgassed using higher-than-normal emission, the upper curve of Fig. 12 was obtained. The BAG also showed some indication of a change in calibration (Fig. 10) but not nearly as large as that exhibited by the magnetron so it is unlikely that the total shift in output was due to changes in the calibration system itself.
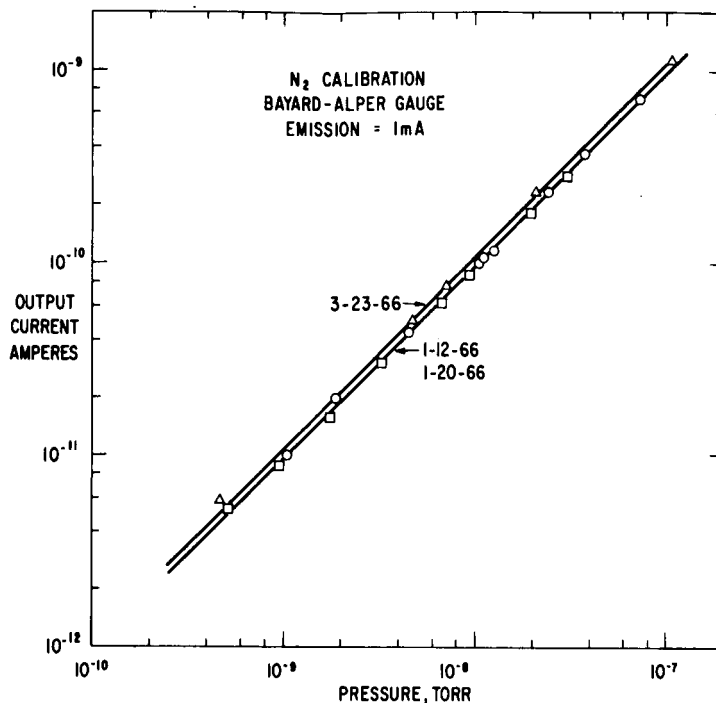
Fig. 10 Calibration curves of Bayard-Alpert gauge at high pressures. The lower curve shows the agreement obtained for two different calibration runs and also the generous amount of overlap between calibrations with V_1 open (O) and V_1 throttled (□). The upper curve was obtained after further bakeout and out-gassing. The departure from linearity at the lowest pressures is caused by the residual or "x-ray" current.
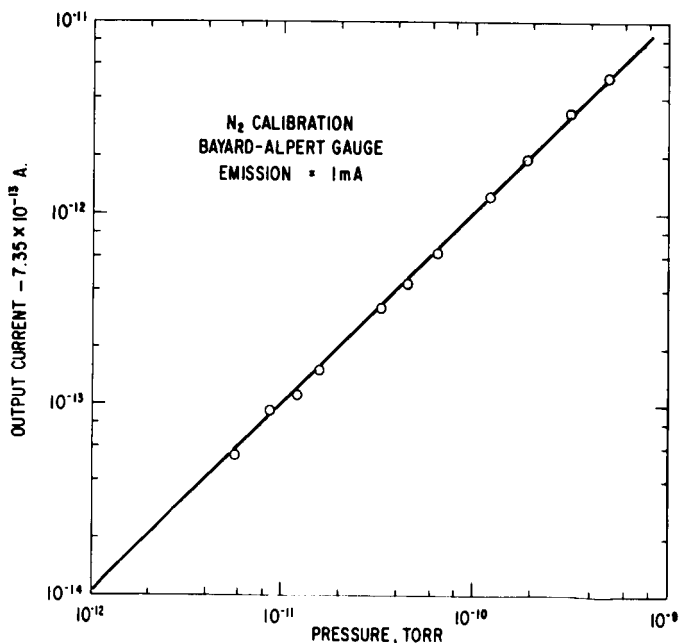
Fig. 11 Calibration curve of Bayard-Alpert gauge at low pressures obtained by sub-tracting residual current from measured output current.
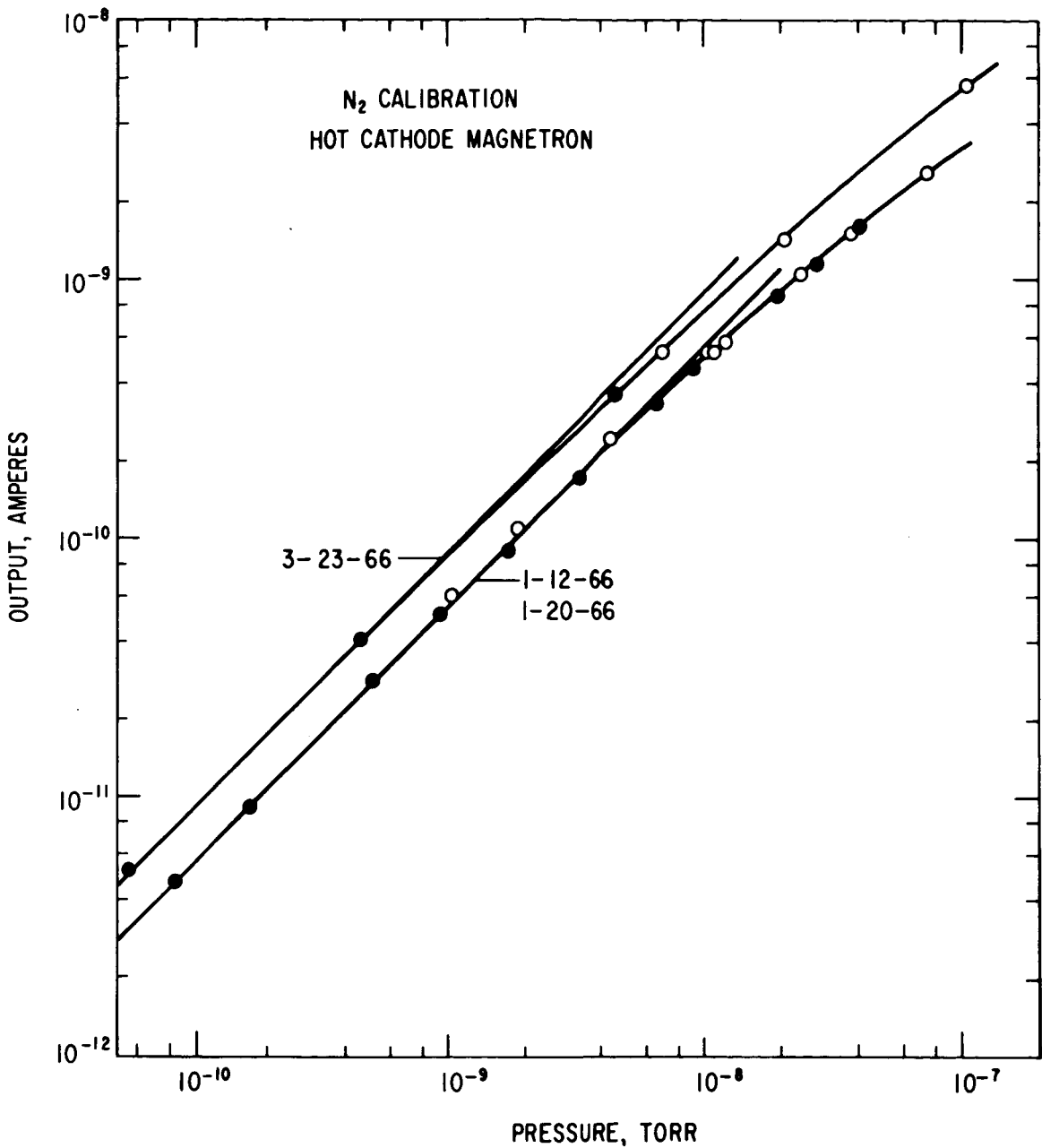
Fig. 12 Calibration curves for hot-cathode magnetron at high pressures. A
bakeout and outgassing occurred between the two curves. Emission = 1 x 10^{-7}
amp: $\bigcirc$ = V_1 open, and $\bullet$ = V_1 throttled.

Prior to this calibration, it was noticed that at the chosen magnet
position, the gauge exhibited bistable operation. At constant pressure, either
of 2 output currents differing by 30% could be obtained depending on the manner
in which operating conditions were achieved, particularly the positioning of the

magnet or the adjustment of the filament emission. For this calibration, the higher mode was chosen. At the time of the first calibration, this phenomenon was not observed but may have been present. Thus, a shift in mode could account for some of the difference in the two calibration curves. The other magnetron gauge also exhibited bistable operation with a current ratio of 1.7. Although this effect was not studied thoroughly, it was clearly pressure dependent and thus may represent a transition stage from a stable mode at high pressures to a different stable mode at lower pressures. For example, the magnetron on the calibration manifold exhibited bistable operation at 10^{-10} torr, but only the low sensitivity mode could be obtained at pressures less than 5×10^{-11} torr.

Oscillations in the gauges were also observed for certain magnet positions. The tendency to oscillate seemed to increase with decreasing pressure. The best position of the magnet was usually located by rotating it until a position was found that was reasonably far from an oscillatory position and yet produced a sensitivity near the maximum. This position, however, did not necessarily prove to be the best position at lower pressures either from the standpoint of freedom from oscillations or for maintaining single-moded operation. There was also some evidence that drastic conditions such as bakeouts or outgassing procedures caused small changes in the operating stability characteristics, but no such changes were observed during normal operation.

Another difficulty encountered at very low pressures was the lack of linearity with pressure. At pressures in the low 10^{-12} torr region, it was noticed that the ion currents were much lower than expected or even slightly negative. The change in ion current with emission also did not exhibit normal behavior. As the emission was increased, the ion current would rise to a maximum and then decrease instead of monotonically increasing. Reduction of the emission to 5×10^{-8} amp restored normal behavior down to the base pressure of about 2.5×10^{-12} torr. The upper curve of Fig. 13 obtained at this time shows good linearity. As the base pressure approached 1×10^{-12} torr, however, the same difficulty arose. Reduction of the emission to 1 to 2×10^{-8} amp (magnet off) appeared to be at least a temporary solution, but it also decreased the output current which was already becoming difficult to measure. A more satisfactory solution was to increase the negative bias on the collector. Apparently, energetic electrons are present which produce a small negative current to the collector. Lafferty noticed a similar phenomenon for low collector bias. By making the collector -90 volts with respect to the filament, normal characteristics are restored. The final operating conditions chosen were: filament +90 volts, anode +390 volts, shield +35 volts and collector grounded. The emission current was reduced as low as was possible without causing a major loss in ion current. For the calibration magnetron, an emission of 1×10^{-8} amp gave an output of about 0.055 amp/torr while the pump magnetron at 5×10^{-8} amp emission gave 0.059 amp/torr. Due to an error in setting the emission, no calibration has been obtained at the 1×10^{-8} amp emission value, but the lower curve of Fig. 13 shows the results obtained at 0.33×10^{-8} amp emission. Calibration at 1×10^{-8} amp emission will be obtained later, but the results should not be significantly different except for the higher output level.
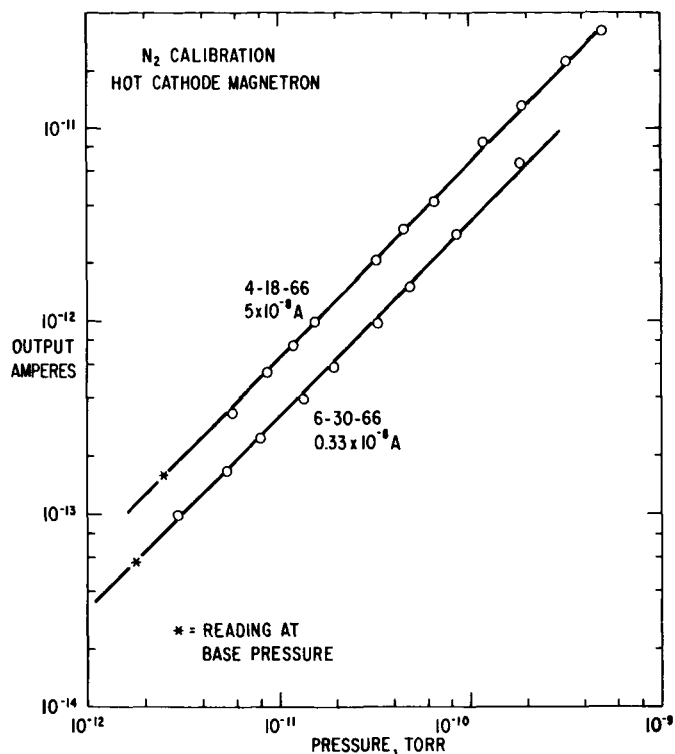
Fig. 13 Calibration curves for hot-cathode magnetron at low pressures. The asterisks show the base pressure at the time and are not calibration points. The voltages applied to the gauge as well as the emission are different for the two runs.

The calculated x-ray level of the gauges depends on the output current measured without a magnetic field and the cutoff emission obtained with a magnet field. Initially the x-ray level corresponded to about 1 to 2 x 10^{-13} torr for uncutoff emission of 1 x 10^{-7} amp or 5 x 10^{-8} amp. This is about an order of magnitude higher than had previously been found for this type of gauge and was due primarily to an abnormally high output current with the magnet off rather than poor cutoff characteristics. At the final operating voltages and currents, however, the x-ray level had been reduced to 3 x 10^{-14} torr for the pump-magnetron and 1.3 x 10^{-14} torr for the calibration-magnetron. These reduced values are not due to a lower yield of x-ray current per ampere of emission as this value stayed remarkably constant throughout the investigation. Instead, it reflects a much better cutoff characteristic (emission ratio = 200) in the case of the pump magnetron and the low emission used (1 x 10^{-8} amp) in the case of the calibration magnetron. It should be pointed out that the term "x-ray current" is used loosely here because the measured residual current did not behave in the predicted manner for changes in magnet position or anode voltage. The nature of this residual current needs further investigation, but because it did not appear to be significant at the present pressure levels, it was not studied further.

3. Triggered Discharge Gauge

The Triggered Discharge Gauge (TDG) was operated according to the manufacturer's recommendations. No attempt was made to adjust the magnet

to a preferred orientation. All discharges at low pressure were initiated by the starting filament. To avoid noise at low pressures, a highly regulated power supply is necessary for the -2 kv anode potential. The only serious difficulty encountered was electrical leakage or field emission to the ion collector after bakeout which necessitated sparking with a Tesla coil. A typical background current obtained at low pressures before the discharge was initiated was -6×10^{-15} amp. The reason for the negative sign of the current has not been ascertained. In any case, this current is only about 10% of the ion current at 10^{-12} torr.

Figure 14 shows the calibration curve obtained for this gauge. The rated output of 2.5 amp/torr occurs at 1×10^{-6} torr. The output current, however, varies approximately as $P^{1.2}$ so that at a pressure of 1×10^{-11} torr, the sensitivity is only 0.1 amp/torr. This makes current readings at low pressures with this gauge about as difficult as with the hot-cathode magnetron gauge. Young has reported finding a similar $P^{1.2}$ behavior.[9, 10]

The output current does not follow a smooth curve with pressure, but exhibits several discontinuous jumps undoubtedly caused by mode changes in the discharge. At some critical pressures, oscillations occur as the mode rapidly changes back and forth. The pressure at which the jump occurs depends on whether the pressure is increasing or decreasing. This leads to a hysteresis-like loop in the calibration curve as indicated at the low-pressure end of Fig. 14. Moreover, points within the loop are also possible depending on how one approaches the final pressure. The lower boundary of the loop was fairly well established by carefully increasing the pressure from the base pressure, avoiding any momentary overpressures. The four points defining the upper part of the loop were obtained by comparing this gauge with the hot-cathode magnetron gauge as the pressure was decreased from a pressure of about 10^{-9} torr. The three square points within the loop were obtained by decreasing the pressure just after the jump started to occur. The other points within the loop were taken before this effect was observed and the proper precautions taken to avoid pressure fluctuations in approaching the final pressure. Some of the scatter in the data at other pressures may be due to the same cause.

The other large jump obtained on increasing the pressure to 10^{-9} torr is shown. A small jump of about 1×10^{-10} amp occurs slightly above this point and probably other small discontinuities are present that were not noticed. Sufficient data were not obtained, however, to show in detail the small deviations from the general trend along the $P^{1.2}$ line.

There was only one occasion when the discharge went out as the pressure decreased into the 10^{-12} torr region. This may have been caused by a temporary failure in the high voltage as it never recurred even at pressures as low as 1×10^{-12} torr.

4. Mass Spectrometer

The ion current sensitivity of the spectrometer was 0.3 to 0.5 torr^{-1} for the tungsten filament. For a normal electron emission of 10^{-4} amp, an ion current of about 4×10^{-5} amp/torr is obtained. The electron multiplier had a gain of 3 to 4×10^7 at 1800 volts giving a total output current of the order of 1000 amp/torr. The sensitivity for the Re LaB$_6$ filament was somewhat less.
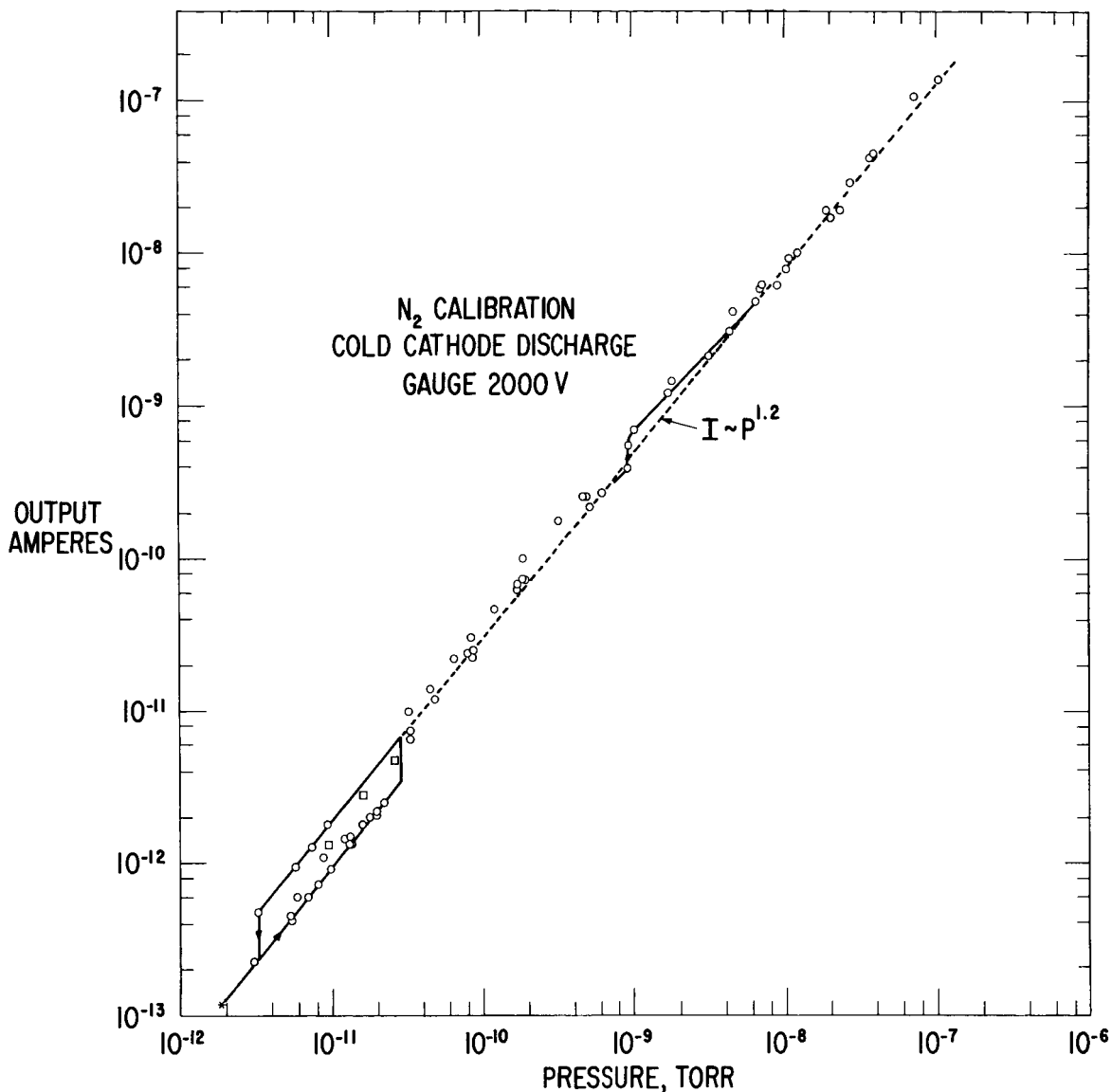
Fig. 14 Calibration curve for the triggered discharge gauge showing the $P^{1.2}$ dependence. See text for explanation of points on hysteresis loop at lowest pressures.

The multiplier background or noise was equivalent to about 2×10^{-16} torr using d-c current measurements or $<10^{-17}$ torr using ion counting techniques. The background of scattered ions (probably F^+), however, produced a noise level equivalent to about 1×10^{-15} torr over portions of the spectrum.

The entrance and exit slits to the analyzer were 0.25 and 0.38 mm, respectively. The resulting peak width at the 10% intensity points was about 0.76 mm or an $M/\Delta M$ of 66.

The major difficulty with the mass spectrometer was not lack of sensitivity or resolution but outgassing due to the hot filament. By thoroughly outgassing the source by electron bombardment from an auxiliary 0.13 mm W filament and reducing the emission to 10^{-5} amp, the outgassing was sufficiently reduced that the sum of the partial pressures (essentially, masses 28 and 2) did not disagree significantly from the total pressure readings of the magnetron and cold-cathode gauges for base pressures of 10^{-12} torr. Also, the readings of the total pressure gauges were not affected by turning the spectrometer on or off.

Figure 15 shows the total output obtained by adding the mass 2 and mass 28 ion currents as a function of the total pressure during a N_2 calibration. The initial readings before adding N_2 were mass 2 = 1.2×10^{-10} amp and mass 28 = 0.6×10^{-10} amp. At the highest pressure, the mass 2 reading had increased to only 2.0×10^{-10} amp. This particular spectrometer maintained linearity up to 10^{-7} torr, the highest pressure used. In between bakeouts the calibration seemed to be quite stable. Neither of the two major peaks, masses 28 and 2, showed any indication of having an appreciable fraction of surface ions at the lowest pressure obtainable.
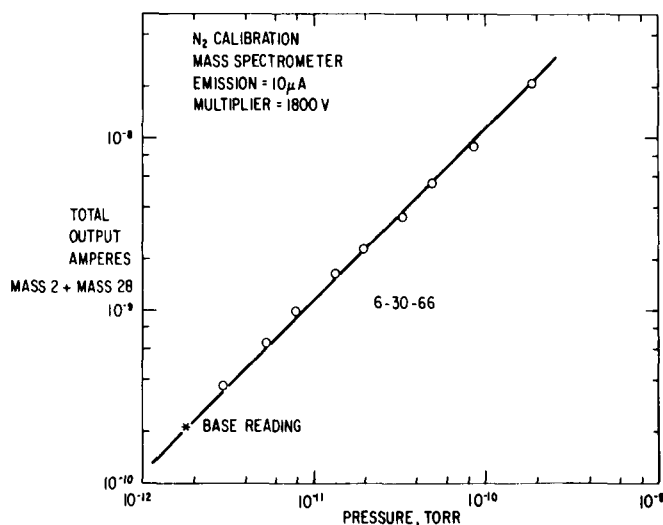
Fig. 15 Calibration curve for mass spectrometer at low pressures obtained by adding the two main gas peaks of the spectrum.

F. Calibration with H_2 and O_2

Calibration runs of an exploratory nature were made with two other gases, H_2 and O_2. No attempt was made at this time to attain maximum accuracy but merely to obtain a reasonable good calibration for H_2, one of the main residual gases present, and to assess the problems in calibrating with O_2.

H_2 behaved normally and the results were about as expected. Figure 16 shows the results for the single run made. The detail shown for the discharge gauge was obtained from a recording made as the pressure was slowly increased. The mass 28 level during the run remained at about 2×10^{-12} torr and there was no evidence of the formation of H_2O. Thus, it can be assumed that the calibration

-18-

Fig. 16 Calibration curves for all gauges using H_2. V_1 throttled. Absolute pressure determined by prior N_2 calibration at same valve setting. BAG readings corrected for residual current. Emission of hot-cathode magnetron $= 5 \times 10^{-8}$ amp.
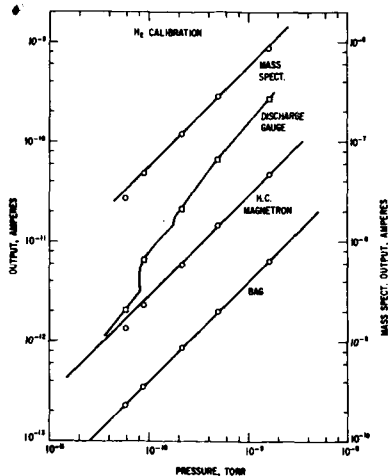
gas was reasonably pure H_2. Table I compares the results for N_2 and H_2 and shows that all gauges have about the same sensitivity ratios for these two gases. Because the sensitivity of the discharge gauge is not constant, the comparison was made both for a constant pressure and a constant current.

TABLE I

Sensitivity (amp/torr)

	N_2	H_2	Ratio H_2/N_2
BAG (1 ma)	0.0105	0.0039	0.37
Hot-cathode magnetron (5×10^{-8} amp)	0.065	.028	.43
Mass spectrometer (1×10^{-4} amp, 1800 v)	1370	550	.40
Discharge gauge (5×10^{-10} torr)	0.42	0.136	.32
Discharge gauge (1×10^{-10} amp)	2.4×10^{-10} torr	7.0×10^{-10} torr	.34

Calibration with O_2 was more difficult, as would be expected for such an active gas. The measurements could not be extended below about 5×10^{-8} torr because flow through the throttled valve was impeded by absorption in the valve. This led to extremely long equilibration times. Even with this valve open, about 1/2 hour was required to obtain a steady reading. The major impurity in the gas in the calibration manifold was mass 28 ($CO + N_2$) which varied from 2% for an O_2 pressure of 1.2×10^{-8} torr to 1% at 8.4×10^{-8} torr. The other impurities were mass 44 (CO_2) which varied from 1.5% to 0.8% and mass 40 (Ar) which was constant at 0.5% (probably an impurity in the O_2 supply).

Only the cold- and hot-cathode magnetrons gave results which appear to be reasonably accurate. The BAG was operated using the ThO_2 coated Ir filament at 1 ma, but as the residual current could not be monitored continuously, the readings were undoubtedly higher than the true gas phase ion current. This was indicated by the fact that for the same pressure the output current was considerably greater for O_2 than for N_2 while just the opposite was true for the magnetron type gauges.

Figure 17 shows the limited data obtained thus far. An earlier run is not included because insufficient time was allowed for equilibration. The N_2 calibration curve is included for comparison. The hot-cathode magnetron emission was 1×10^{-7} amp. The points indicated by diamonds were taken by decreasing the pressure after the highest pressure was reached. The highest of these at 2.5×10^{-8} torr agrees within 2% with the reading taken at the same pressure, but on the way up in pressure. The lowest of these points agrees reasonably well considering that the correction for back pressure P_2 was 20% of the total pressure. This agreement indicates that equilibrium must have been achieved.
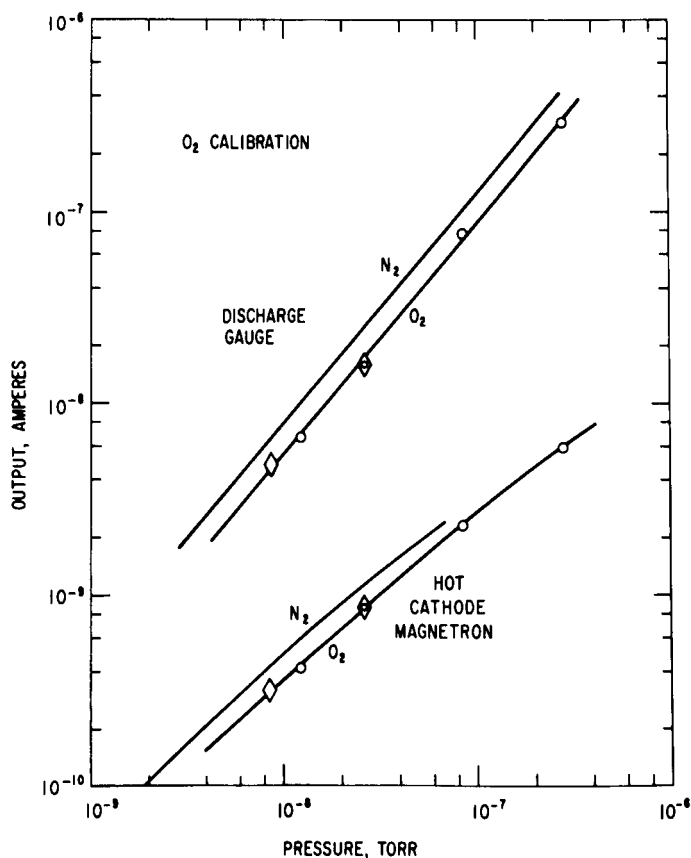

Fig. 17 Calibration curves obtained with O_2. The applicable N_2 calibration is also shown for comparison. Emission of hot-cathode magnetron was 1×10^{-7} amp (magnet off): ○ = pressure increasing, and ◊ = pressure decreasing.

G. Discussion of Errors

The errors associated with this calibration procedure have not been well determined because the main emphasis was on attaining low calibration pressures and proper gauge operation rather than tracking down and reducing all the small errors. In general, however, efforts were made to keep the errors involved in determining the absolute pressure, P_1 down to the level of about 1 to 2%. This would include the measurement of C_1, C_2, and P_M. The error in P_2 probably exceeds 1% but the resulting error in P_1 should not exceed 1%.

The greatest known error lies in the determination of P_M. While ordinary care was taken in reading the McLeod gauge, a cathetometer was not used. In addition, the usual errors associated with McLeod gauges such as sticking Hg, capillary depression, etc. were undoubtedly present and the 1% to 2% level of precision probably was not reached until P_M was about 10^{-2} torr. The manufacturer's calibration of the gauge was not checked, but as stated earlier, good agreement was obtained between flow measurements using this gauge and the calculated conductance of a glass capillary tube.

Considering these known sources of errors and the reproducibility of successive calibrations, an over-all error of $\pm$ 5% in the absolute value of the pressure is believed to be a conservative estimate. There are other sources of error, however, which may exist but which have not been determined or are difficult to estimate. For example, C_1 may have undergone dimensional changes during bakeout. This will be checked later by flow measurements. Pressure variations within the calibration region due to directed flow may be present. This could be detected by interchanging stable gauges among the various parts. This would not, however, reveal any directed flow from C_1 to C_2. These types of errors are believed to be small but may not be insignificant.

The above analysis applies only to the primary calibration when C_1 is the determining conductance. Successively lower pressure ranges obtained by throttling V_1 have the additional errors associated with what amounts to lining up a series of overlapping segments of the calibration curve. The averaging effect obtained by considering all the gauges helps to reduce the error involved, but each step probably adds a few per cent of uncertainty in the calculated pressure. The range of each step allowing for overlapping between steps is about a 100 to 1 in pressure. Thus, it takes about 2 steps to reach the 10^{-12} torr region.

As the calibration pressure approaches the base pressure, the corrections due to P_2 and $(P_1^0 - P_2^0)$ become the major source of error. Indeed, P_2 can only be estimated by assuming that the magnetron measuring P_2 is linear below the lowest calibration point. As a consequence, calibration points obtained only factors of 2 or 3 above the base pressure can be considered only approximations. If all the gauges indicate normal performance at these pressures and the points so determined follow the extrapolated calibration curve, the corrections are probably valid.

The electrometers used to measure the output currents of the gauges were also calibrated to within about 1% to 2%, primarily to ensure that the relative values of the currents for any one gauge would be accurate. The

various other voltages and currents (such as emission currents) were maintained constant but no attempts were made to verify their absolute values. The instruments used however should have been accurate to about $\pm 3\%$. For this study, maximum accuracy in the absolute value of the gauge sensitivity was not deemed necessary.

H. Conclusions

The results obtained indicate that the method of calibration gives satisfactory results down to pressures approaching the base pressure of the system. The most unsatisfactory feature revealed thus far is the high base pressure and the difficulty experienced in obtaining this level of pressure. On the other hand, the base pressure of 5×10^{-13} torr at the He pump is believed to be accurate to within at least a factor of 2 while some of the reported pressure values of 10^{-13} torr or less were obtained with uncalibrated discharge gauges. Linear extrapolation of a calibration at 10^{-6} torr down to 1×10^{-12} torr could lead to errors of a factor of 20 to 40 for the GE discharge gauge and probably even larger errors for the Redhead or Kreisman gauges.

Comparison of the three gauges calibrated (BAG excepted) shows that under the proper operating conditions and suitable calibration, all will measure pressures of 10^{-12} torr with each having its own set of advantages and disadvantages. The discharge gauge is the most convenient to operate, showed no detectable changes in calibration and the least amount of outgassing. However, because of the high voltage used it is probably more susceptible to leakage or field emission currents. Mode changes, nonlinearity and hysteresis limit the accuracy to about a factor of 2. The hot-cathode magnetron is intermediate in terms of ease of operation and degree of outgassing, neither of which are serious problems. It maintains its calibration under normal operating conditions but its behavior after bakeout and outgassing needs further investigation. Oscillations and mode changes, while present under certain conditions, can usually be circumvented so that linear unambiguous readings are obtained. Once calibrated, it probably is the most accurate of the gauges but at this stage of development, calibration should be carried down to the lowest pressure to be measured. Until more experience is obtained with these gauges, the assumption of linearity from a higher calibration point may lead to significant errors. The proper choice of magnet configuration, field strength, field shape, and operating voltages would probably alleviate if not eliminate some of the problems encountered at pressures below 10^{-10} torr.

The mass spectrometer provides the most information but is also the most difficult to operate if peak performance is to be obtained. More variables affect the sensitivity and the calibration must be checked frequently, especially after a bakeout. Outgassing is more difficult but not inherently so. Probably the ideal instrumentation for measuring low pressures is a combination of a stable low-outgassing total pressure gauge and a mass spectrometer.

II. MAGNETRON ION SOURCE

A. Introduction

The primary goal of this phase of the work was to develop a magnetron-type ion source for a quadrupole mass spectrometer which would have substantially higher output ion currents than the conventional ion source without resorting to large electron emission currents. The purpose was to produce a spectrometer that would measure very low pressures without the added complications and instabilities associated with electron multipliers nor the outgassing associated with large electron currents. Conventional electron bombardment ion sources with a sensitivity of about 10 torr $^{-1}$ are capable of producing about 10^{-2} amp/torr of unfocused ion current at 1 ma emission, but normally the input to the analyzer is 10^{-3} to 10^{-4} amp/torr. For measuring pressures below 10^{-10} torr, even lower electron emissions are desirable. Hot-cathode magnetron ion gauges with a sensitivity of 10^6 torr^{-1} or greater have been developed that yield unfocused ion currents of almost 0.1 amp/torr for 10^{-7} amp electron emission.[1,2] What portion of this ion current can be focused down to meet the requirements of the analyzer or what the spread in ion energies would be are not known, however.

A magnetron ion source would be expected to have several conflicting requirements. For efficient focusing, a small ionization region would be desirable, but for maximum total ion current generated in the ionization region, a large ionization region, a high magnetic field, high voltages, and a high electron emission would probably be helpful. High voltages, however, would tend to increase the spread in ion energies, while for stability one would prefer a low electron emission and low magnetic field. The over-all problem therefore was to determine the magnitude, spatial distribution, and energy distribution of the focused ion current as a function of the various design and operating parameters.

Prior use of a hot-cathode magnetron as an ion source had been restricted to a very small ion source constructed for a magnetic sector mass spectrometer. The construction details are shown in Fig. 18. The ionization region defined by the inside bore of the cylindrical magnet was about 0.63 cm diameter by 2 cm long. The magnetic field was 400 to 500 gauss, anode voltage 25 to 50 volts with respect to the filament, and the end shields at -200 volts. The total ion current yield was about 1×10^{-3} amp/torr at 1 μa emission with about 50% of the ions capable of being focused through a 0.25 mm slit. The ion energy spread was probably less than 10 volts as the resolution of the spectrometer was essentially normal. Higher electron emissions did not greatly increase the ion current.

B. Experimental Ion Sources and Results

Ideally, the ion source for a mass spectrometer should not be developed separately from the analyzer. For these initial studies, however, it was thought that some useful information could be obtained from the source alone by determining the ion current yield meeting the requirements imposed by a particular mass spectrometer design. These requirements furnished by NASA were that the ions pass through a 0.51 mm hole with a 1/2 angle of divergence of 1.3° and an energy of 350 volts.

0.010" SLIT

0.040" SLIT

FOCUS
ELECTRODES

MAGNET
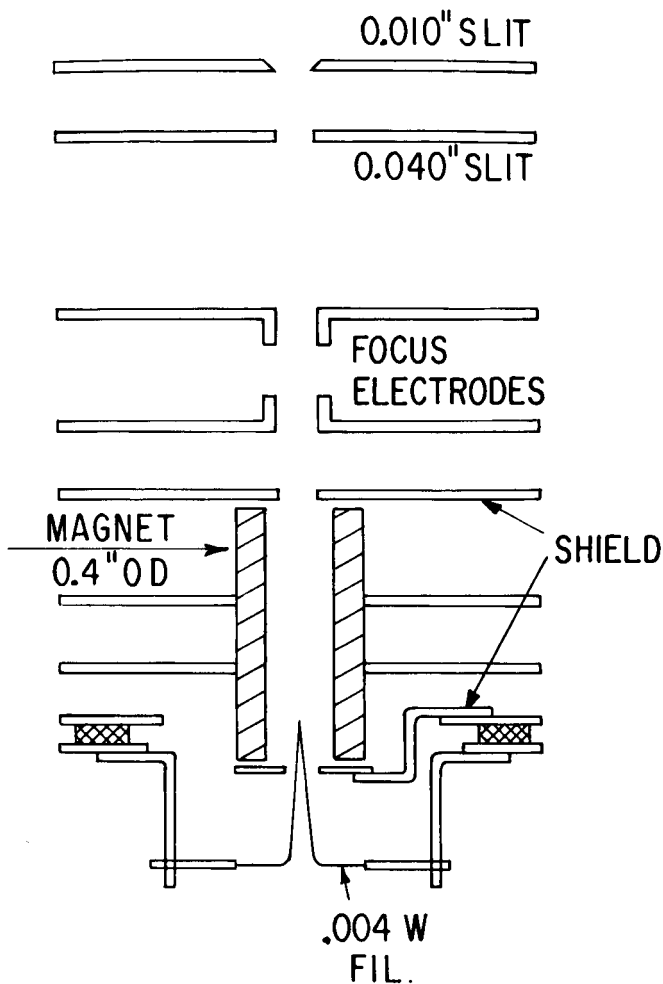0.4" OD

SHIELD

.004 W
FIL.

Fig. 18 Construction of 6.3-mm-diameter
magnetron ion source for magnetic sector
mass spectrometer. The apertures in the
shield are circular while those in the focus
electrodes are rectangular (large slits).

Two different ion sources as shown in Fig. 19 were constructed. In one, (A) the ionization region was essentially the same as in the magnetron ionization gauges developed by Lafferty. Thus, properties of the source itself would be known more extensively than other geometries, but the large diameter might make efficient focusing difficult. The anode was 2.5 cm diameter and 4.5 cm long. The back shield electrode was a 2.5-cm-diameter disk with a 3.2 mm aperture to accommodate the 0.13 mm tungsten filament. The filament projected about 1.6 cm inside the anode. Originally the front shield was identical to the back shield, but the aperture through which the ions are withdrawn was changed later. The structure shown together with the ion optics was mounted in a close-fitting glass tube and the magnetic field supplied by an external permanent magnet 5 cm long. The glass tube was pumped by a small ion pump.

The small source (B) was a compromise between the large diameter source and the low yield 0.63-cm-diameter source mentioned previously. A 1.25 cm inside-diameter permanent magnet served as the anode. The outside diameter was 2.5 cm and the length 3.75 cm. The two shields and the filament were essentially the same as for the large source. The whole unit together with the ion optics was mounted off the flange of a 10-cm-diameter stainless steel cylinder pumped by a 4-inch oil diffusion pump.

Ion generation within the magnetic field region was essentially independent of the ion optics used to draw out and focus the ion beam. The position of the magnet and the voltages applied to the anode and shields which produced the greatest total ion current corresponded closely to the conditions which produced the greatest ion current to the final collector. For the 2.5 cm diameter ion
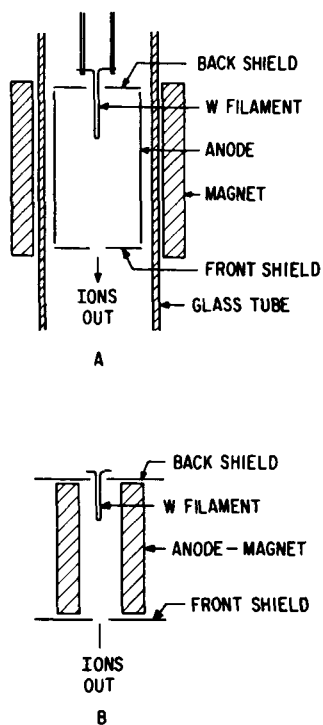
Fig. 19 Construction
of 1.25- and 2.5-cm-
diameter magnetron
ion sources.

source, the total ion yield at a pressure of about 1×10^{-7} torr of N_2 and 1×10^{-5} amp emission (no magnetic field) was approximately 0.3 amp/torr. The yield was not greatly dependent on emission between 10^{-7} and 10^{-4} amp.

The anode voltage used was typically 200 to 300 volts with a magnetic field of about 450 gauss. The ion current was a maximum for shield voltages of about -250 volts. Operating characteristics were about the same as those for the magnetron ionization gauge. The greater ion yield is due to the larger magnetic field, emission current and shield voltages used. At lower pressures, these values may have to be reduced to obtain stable nonoscillatory operation.

The 1.25 cm source produced about 0.05 amp/torr for an emission of 1×10^{-7} and a pressure of 1 to 2×10^{-7} torr. (Because the magnet could not be removed, this emission value is for the magnetic field on, but by using high anode voltages the total emission was estimated to be three to six times greater.) For a shield voltage of -600 volts with respect to the filament, the ion current peaked at an anode voltage of +75. (The ratio of the ion yields for the two sources corresponds approximately to their volume ratio of 5 to 1.) The sensitivity increased with decreasing pressure so that at the limit of the unbaked system, 2×10^{-8} torr, a yield of 0.24 amp/torr was obtained, but this may be somewhat high because of outgassing by the hot filament.

The first set of ion optics chosen was simply two apertures of 4.8 mm diameter as shown in Fig. 20(a). The lower three apertures served to define the ion beam according to the design specifications and were used in all later modifications as well. By monitoring the ion current to these electrodes, one could determine approximately how well the source was focusing the ion beam to meet these requirements. Ion currents to the other electrodes were also measured to determine the over-all efficiency of the source in producing ions and where the major losses of ions were occurring. This first set of ion optics was relatively inefficient, especially for the large diameter source. Only about 0.7% of all the ions passed through the first defining aperture (0.76 mm diameter) for the 2.5 cm source and 4% for the 1.25 cm source. For the 1.25 cm source, the ion current to the collector corresponded to 3×10^{-4} amp/torr.

The second set of ion optics as shown in Fig. 20(b) gave a considerably better performance. The sum of the ion currents to the collector and the adjacent electrode (the ion current passing through the 0.51 mm aperture) amounted to 2 to 3×10^{-3} amp/torr for the 2.5 cm source and about 1×10^{-3} amp/torr for the 1.25 cm source. This corresponds to 1% and 2%, respectively, of the total ion current generated. For the 2.5 cm source, only about 1/4 of the total ions were withdrawn through the 3.2 mm aperture in the end shield, the remainder going equally to the two end shields. For the smaller source, 1/2 of the ions were

FRONT SHIELD

3.2 }4.8
4.8 }6.4
4.8
     }19
0.76
0.51 }6.4
0.76 }6.4

COLLECTOR

FRONT SHIELD

3.2
1.6 |4.8| }4.8
1.6 |4.8| }6.4
1.6
     |6.4| }11.1
3.2 | |

12.5
1.6
12.5   }14.3
1.6
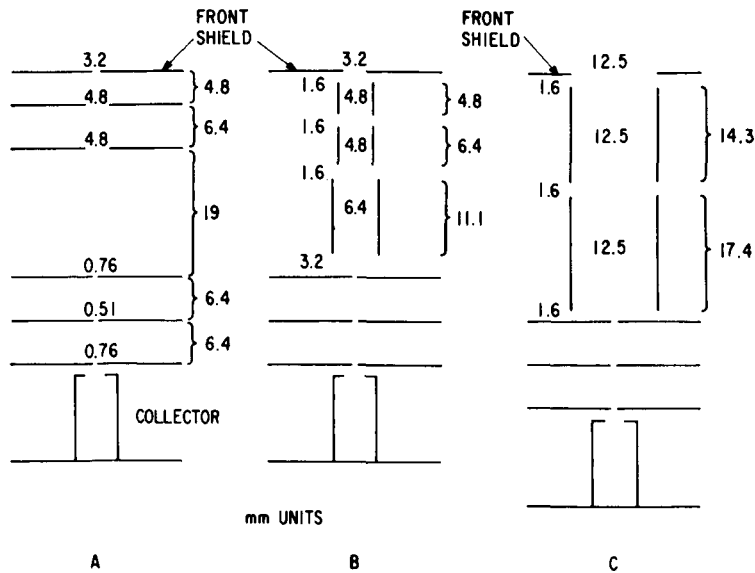12.5   }17.4
1.6

mm UNITS

A   B   C

Fig. 20 Ion focusing systems used with magnetron ion sources showing aperture and cylinder diameters. The lower four electrodes are common to all three systems and are for measuring beam properties.

withdrawn with almost all of the remainder going to the back shield. Thus, the greater withdrawal efficiency of the small source partially compensates for the greater efficiency of the larger source in generating ions.

The efficiency after withdrawal was about the same for both sources. About 60% of the withdrawn ions arrive at the first defining aperture, 20% to 25% of these pass through this aperture and a similar fraction passes through the second defining aperture.

In an effort to improve the withdrawal of ions from the large source, the opening in the shield was enlarged from 3.2 to 12.5 mm. The ion optics were also enlarged to match the larger opening as shown in Fig. 20(c). With this arrangement, the ion generation rate increased to 0.7 amp/torr for 2.5×10^{-7} amp emission (before cutoff) and 1×10^{-7} torr. Essentially none of the ions hit the front shield, 42% were collected at the back shield and 32% were collected on the first focus cylinder. These results suggest that the ionization region had increased so as to include a portion of the volume within the focus cylinder. About 1/4 of the total ions arrived at the first aperture, but only 9% of these passed through the aperture and only 8% of the remainder passed through the next aperture. Because of this significantly poorer focusing, the net current collected was 1.4×10^{-3} amp/torr or 0.2% of the total ions generated. Increasing the emission a factor of 10 increased the ion current by 3 to give 4×10^{-3} amp/torr.

No detailed measurements of ion energies were made for any of the sources but some crude retarding potential measurements on the 2.5 cm source indicated that the energies corresponded more nearly to ion formation at filament potential than to anode potential. Most of the ions were in the range 0 to 50 volts above filament potential. The ion energy spread for the 1.25 cm source is undoubtedly smaller.

C. Conclusions

The results obtained so far show that ion currents of 1 to 5×10^{-3} amp/torr are readily obtainable at pressures of 1×10^{-7} torr from a magnetron type ion source. With further improvements and at lower pressures, ion currents of 1×10^{-2} amp/torr probably can be attained. However, instabilities and oscillations at lower pressures or excessive ion energy spread may force a lowering of the magnetic field or source voltages. This would tend to lower the ion current yield.

On the other hand, a large percentage of the ions are lost in defining the ion beam and considerably greater net ion currents would be obtained if the entrance requirements for the quadrupole analyzer could be relaxed.

III. FABRICATION OF HOT-CATHODE MAGNETRON GAUGES

A. Introduction

One hot-cathode magnetron gauge of conventional design was delivered to the contracting officer in July 1965 and was found not suitable for high vibration applications. Three flight-model hot-cathode magnetron gauges have been constructed since, of metal and ceramic. A new radial header design was used which allows more supporting leads for added sturdiness and a shorter exhaust tubulation. A lanthanum hexaboride cathode is used as an electron emission source in all of the gauges. One of the flight-model gauges is terminated with a glass tubulation and is being delivered evacuated and sealed off. A fifth gauge was constructed of glass with identical electrode structures. This gauge is also being delivered sealed off under vacuum. A sixth gauge of conventional design is to be furnished after calibration.

B. Gauge Fabrication

The flight-model magnetron gauge consists of a 347 stainless steel header with nine (9) ceramic feed-throughs located radially. They are brazed into the header with a silver-copper eutectic alloy. The feed-throughs are manufactured and brazed into place by Ceramaseal, Incorporated. The support leads are 1.25-mm-diameter 347 stainless steel rod. The radial arrangement of nine leads lends itself to a sturdier design by permitting three-point support for each electrode and also results in a shorter exhaust tubulation (see Figs. 21 and 22). The internal electrodes of the gauge are all made of stainless steel except for the filament which is formed from rhenium wire and coated with LaB_6. Two gauges were assembled with 0.025-mm-diameter filaments and a third was constructed with a 0.013-mm-diameter filament. The collector consists of a 2.5-cm-diameter disk of 0.025-mm-thick stainless steel. The anode and shield are fabricated from mesh and are reinforced with a stainless steel ring or bands at the edges for lead attachment. The open mesh is used for two reasons. One reason is to reduce the mass of both electrodes, thus reducing their intrinsic low-frequency resonances (vibration tests were conducted and will be discussed later). The other reason is that the open-mesh permits high conductance between gauge and vacuum under study and provides quick response to transient pressure changes.

The emitter material is applied cataphoretically after the rhenium filament is mounted in place. A suspension of finely divided lanthanum hexaboride powder in ethyl alcohol is used for coating. The LaB_6 coating is then sintered at 1500°C in vacuum for approximately 20 minutes. In the past on occasions the boride coating has been known to flake off. This problem is being investigated and it has been learned that free boron or boron oxide (B_2O_3) is present in the LaB_6 powder supplied to us. During sintering, rhenium borides Re_7B_3 and ReB_2 are formed. The borides are visible as a grayish film underneath the LaB_6 layer and cause the emitter coating to flake off. We have attempted to eliminate the boron and boron oxide in two ways. First, the LaB_6 powder is vacuum fired in a graphite crucible for 2 hours at 1800°C. The more volatile B_2O_3 should evaporate off under these conditions. To eliminate the boron, the LaB_6 powder is mixed
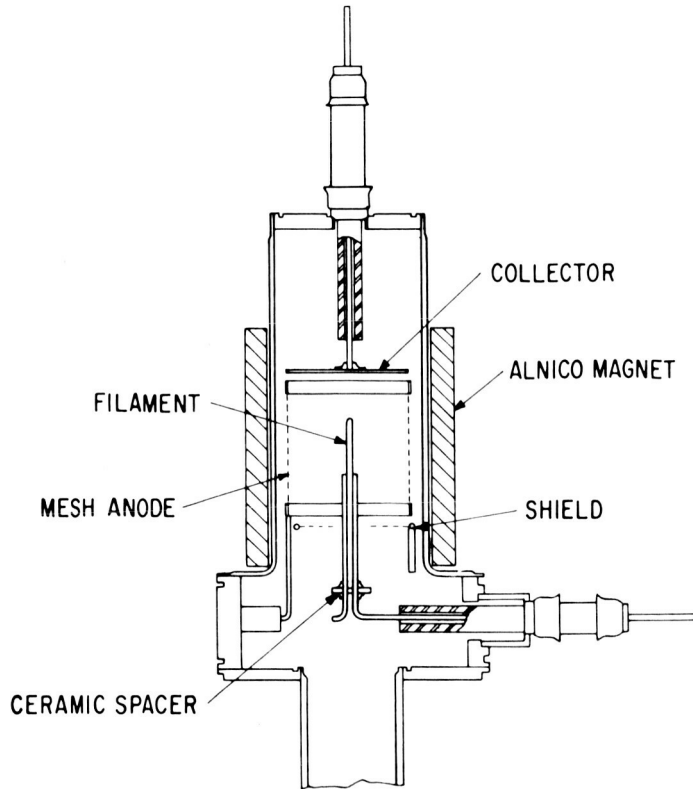
Fig. 21 Construction of flight model of hot-cathode magnetron gauge.

COLLECTOR

ALNICO MAGNET
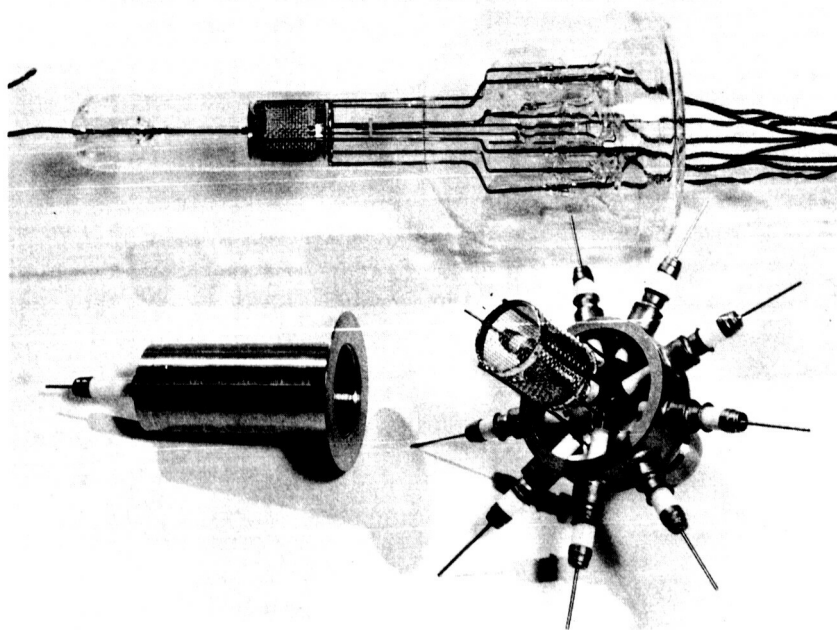
FILAMENT

MESH ANODE

SHIELD

CERAMIC SPACER

Fig. 22 Photograph of flight model and all-glass versions of the hot-cathode magnetron gauge.

with ethyl alcohol, stirred, and then allowed to settle for approximately 30 minutes. The remainder of the powder still in suspension is poured off. It is reasonable to assume that the lighter boron powder present will tend to stay in suspension longer and be selectively removed by repeated decanting. Six rhenium filaments have been coated with LaB_6 material processed in this manner and vacuum sintered as high as 1600°C. Only one flaked after 3 days. However, it was a filament that had been used previously and might have been contaminated with rhenium borides. The other five cathodes were constructed of new rhenium wire and are still in excellent condition after more than 1 week.

A magnetron gauge was also constructed with a glass envelope for outgassing rate studies (see Fig. 22). The envelope is FN glass terminated with a Pyrex-exhaust tubulation. All the metal parts, except the support leads, are a duplicate of those used in the flight-model gauge. The filament leads are similarly supported with a small ceramic insulator. A 0.013-cm-diameter rhenium filament was used in this gauge. All the stainless steel metal parts were vacuum fired before assembly. After completion, the gauge was exhausted and baked out at 400°C for 12 hours. The metal electrodes were outgassed further by electron bombardment making use of the cathode emission. The gauge was sealed off at a pressure of 1.0×10^{-9} torr.

C. Vibration Testing

The magnetron gauge structure shown in Fig. 21 was submitted to vibration tests according to Explorer 17 subassembly specifications. In the axial direction, anode resonances were found with an acceleration level of 3G at 120 cps and from 163 to 170 cps. The shield resonance was found from 205 up to 271 cps. These resonant vibrations were not serious but did produce audible noise. Filament vibrations did not occur in this position.

In the thrust direction, which is perpendicular to the axis, the vibrations were more severe. The mesh anode resonated at 118 to 126 cps and an acceleration level of 15G. Maximum resonance occurred at 126 cps. Resonance was observed again at 164 cps but were much less severe. The shield resonated at 40 to 59 cps, 74 to 80 cps, and again at 210 to 224 cps. Filament resonance was observed at 80 cps, 140 cps, and from 415 to 445 cps at an acceleration level of 11G. The strongest vibrations occurred at the higher frequencies. Following the test, the gauge structure was carefully inspected and found to be in excellent condition. The lead spot welds were undamaged and the alignment of parts was unchanged. Some of the lanthanum boride coating flaked off the bottom of the rhenium filament. However, microscopic inspection revealed a grayish film on the wire underneath the LaB_6 which probably would have caused flaking sooner or later. The new coating solution now being used should prevent this from occurring again.

ACKNOWLEDGMENT

REFERENCES

1. J.M. Lafferty, J. Appl. Phys., 32, 424 (1961).

2. J.M. Lafferty, Trans. 7th AVS Vac. Symp., Pergamon Press, New York (1961), p. 97.

3. F. Feakes and F.L. Torney, Trans. 10th AVS Vac. Symp., The Macmillan Co., New York (1964), p. 257.

4. P.J. Bryant, W.W. Longley, and C.M. Gosselin, J. Vac. Sci. Tech., 3, 62 (1966).

5. W. Kreisman, GCA Tech. Rept. 64-17-N (November 1964).

6. W.D. Davis, Trans. 10th AVS Vac. Symp., The Macmillan Co., New York (1964), p. 253.

7. W.D. Davis and T.A. Vanderslice, Trans. 7th AVS Vac. Symp., Pergamon Press, New York (1961), p. 417.

8. W.D. Davis, Trans. 9th AVS Vac. Symp., The Macmillan Co., New York (1963), p. 363.

9. J.R. Young and F.P. Hession, Trans. 10th AVS Vac. Symp., The Macmillan Co., New York (1964), p. 234.

10. J.R. Young, J. Vac. Sci. Tech., 2, 283 (1965).

NASA SCIENTIFIC AND TECHNICAL PUBLICATIONS

TECHNICAL REPORTS: Scientific and technical information considered important, complete, and a lasting contribution to existing knowledge.

TECHNICAL NOTES: Information less broad in scope but nevertheless of importance as a contribution to existing knowledge.

TECHNICAL MEMORANDUMS: Information receiving limited distribution because of preliminary data, security classification, or other reasons.

CONTRACTOR REPORTS: Technical information generated in connection with a NASA contract or grant and released under NASA auspices.

TECHNICAL TRANSLATIONS: Information published in a foreign language considered to merit NASA distribution in English.

TECHNICAL REPRINTS: Information derived from NASA activities and initially published in the form of journal articles.

SPECIAL PUBLICATIONS: Information derived from or of value to NASA activities but not necessarily reporting the results of individual NASA-programmed scientific efforts. Publications include conference proceedings, monographs, data compilations, handbooks, sourcebooks, and special bibliographies.

Details on the availability of these publications may be obtained from:

SCIENTIFIC AND TECHNICAL INFORMATION DIVISION

NATIONAL AERONAUTICS AND SPACE ADMINISTRATION

Washington, D.C. 20546